



|                  |   |
|------------------|---|
| Title            | The Join CaMgSi <sub>2</sub> O <sub>6</sub> -CaAl <sub>2</sub> SiO <sub>6</sub> -CaFe <sup>3+</sup> AlSiO <sub>6</sub> in air and its Bearing on Fassaitic Pyroxene |
| Author(s)        | Onuma, Kosuke; Yagi, Kenzo  |
| Citation         | Journal of the Faculty of Science, Hokkaido University. Series 4, Geology and mineralogy, 16(4), 343-356  |
| Issue Date       | 1975-02   |
| Doc URL          | <a href="http://hdl.handle.net/2115/36037">http://hdl.handle.net/2115/36037</a>   |
| Type             | bulletin (article)  |
| File Information | 16(4)_343-356.pdf   |



[Instructions for use](#)

THE JOIN  $\text{CaMgSi}_2\text{O}_6$ - $\text{CaAl}_2\text{SiO}_6$ - $\text{CaFe}^{3+}\text{AlSiO}_6$   
IN AIR AND ITS BEARING  
ON FASSAITIC PYROXENE

*by*

Kosuke Onuma and Kenzo Yagi

(with 1 table and 9 text-figures)

(Contribution from the Department of Geology and Mineralogy,  
Faculty of Science, Hokkaido University, No. 1378)

*Abstract*

Phase equilibrium diagram of the join  $\text{CaMgSi}_2\text{O}_6$ - $\text{CaAl}_2\text{SiO}_6$ - $\text{CaFe}^{3+}\text{AlSiO}_6$  was determined by the ordinary quenching method in air at 1 atm. One five-phase assemblage and three four-phase assemblages (univariant and divariant at constant pressure and constant  $p\text{O}_2$ ) were confirmed. The univariant assemblage is clinopyroxene<sub>ss</sub> + anorthite + melilite<sub>ss</sub> + spinel<sub>ss</sub> + liquid. Because of the complex solid solution of clinopyroxene, melilite, and spinel the crystallization ceases before invariant point is reached and the final phase assemblage in the  $\text{CaMgSi}_2\text{O}_6$ -rich region is clinopyroxene<sub>ss</sub> + anorthite + melilite<sub>ss</sub>, and that in the  $\text{CaMgSi}_2\text{O}_6$ -poor region clinopyroxene<sub>ss</sub> + anorthite + melilite<sub>ss</sub> + spinel<sub>ss</sub>. The clinopyroxene<sub>ss</sub> field increases with increasing  $\text{CaFe}^{3+}\text{AlSiO}_6$  content. The clinopyroxene<sub>ss</sub> in the join is discussed, with special reference to its bearing on the natural fassaitic pyroxene from alkalic volcanic rocks.

**Introduction**

In the previous paper (Onuma and Yagi, 1971) we pointed out that main constituent molecules of the pyroxene in understaturated alkalic rocks (nepheline-and/or melilite-bearing rocks) are  $\text{CaMgSi}_2\text{O}_6$  (Di),  $\text{CaTiAl}_2\text{O}_6$  (Tp),  $\text{CaAl}_2\text{SiO}_6$  (calcium-Tschermak's molecule, CaTs), and  $\text{CaFe}^{3+}\text{AlSiO}_6$  (ferri-aluminium-Tschermak's molecule, FATs). In his study of fassaitic augite in alkali basalt Huckenholz (1973) showed that  $\text{Fe}^{3+}$  or  $\text{Fe}^{3+} + \text{Al}$  in excess of Na is incorporated in the diopside structure as  $\text{CaFe}_2^{3+}\text{SiO}_6$  (ferri-Tschermak's molecule, FTs) and FATs.

From the viewpoint above mentioned, the system Di-CaTs-FATs-Tp, which is now under the investigation by the authors, is important to understand the

role of the pyroxene in the differentiation of alkalic rocks. In the present paper, the data of the join in the system Di-CaTs-FATs are presented and the clinopyroxene in the join is discussed with special reference to its bearing on the natural fassaitic pyroxene from alkalic volcanic rocks.

### Experimental Results

In the present investigation ordinary quenching method was employed in air at 1 atm. The starting material was prepared by complete crystallization of homogeneous glass at 900°C. The furnace used in quenching experiments was regulated to a precision of  $\pm 1^\circ\text{C}$ . Pt-Pt<sub>87</sub>Rh<sub>13</sub> thermocouples used to measure the temperature were calibrated at the standard melting points of Au, 1062°C and diopside, 1931.5°C (the Geophysical Laboratory temperature scale). The results of quenching experiments are given in Table 1.

Table 1. Results of the queching experiments of the join  
CaMgSi<sub>2</sub>O<sub>6</sub>-CaAl<sub>2</sub>SiO<sub>6</sub>-CaFe<sup>3+</sup>AlSiO<sub>6</sub>

| Composition (wt.%) |      |      | Temp.<br>(°C) | Time<br>(hrs.) | Results                            |
|--------------------|------|------|---------------|----------------|------------------------------------|
| Di                 | CaTs | FATs |               |                |                                    |
| 80                 | 10   | 10   | 1335          | 2              | gl                                 |
|                    |      |      | 1330          | 2              | cpx, gl                            |
|                    |      |      | 1220          | 72             | cpx, gl                            |
|                    |      |      | 1200          | 72             | loose powder, cpx only             |
| 70                 | 20   | 10   | 1305          | 1              | gl                                 |
|                    |      |      | 1300          | 2              | cpx, gl                            |
|                    |      |      | 1220          | 72             | cpx, an, gl                        |
|                    |      |      | 1200          | 72             | loose powder, cpx, an, mel?        |
| 60                 | 30   | 10   | 1265          | 16             | gl                                 |
|                    |      |      | 1260          | 4              | cpx, gl                            |
|                    |      |      | 1250          | 18             | cpx, trace an, gl                  |
|                    |      |      | 1220          | 72             | barely fritted cake, cpx, an, mel? |
|                    |      |      | 1200          | 72             | loose powder, cpx, an, mel         |
| 57                 | 33   | 10   | 1265          | 2              | gl                                 |
|                    |      |      | 1260          | 2              | an, gl                             |
|                    |      |      | 1250          | 16             | an, gl                             |
|                    |      |      | 1245          | 46             | cpx, an, gl                        |
|                    |      |      | 1240          | 42             | cpx, an, gl                        |
|                    |      |      | 1230          | 46             | cpx, an, mel, gl                   |
|                    |      |      | 1200          | 72             | loose powder, cpx, an, mel         |
| 53                 | 37   | 10   | 1250          | 16             | an, gl                             |
|                    |      |      | 1245          | 46             | an, cpx, sp, gl                    |
|                    |      |      | 1240          | 42             | an, cpx, sp, gl                    |
|                    |      |      | 1230          | 46             | an, cpx, sp, mel, gl               |
|                    |      |      | 1200          | 72             | loose powder, an, cpx, sp, mel     |

Table 1. continued

| Composition (wt.%) |      |      | Temp.<br>(°C) | Time<br>(hrs.) | Results                        |
|--------------------|------|------|---------------|----------------|--------------------------------|
| Di                 | CaTs | FATs |               |                |                                |
| 50                 | 40   | 10   | 1310          | 1              | gl                             |
|                    |      |      | 1305          | 16             | sp, gl                         |
|                    |      |      | 1300          | 2              | sp, gl                         |
|                    |      |      | 1295          | 2              | sp, an, gl                     |
|                    |      |      | 1250          | 18             | sp, an, gl                     |
|                    |      |      | 1245          | 24             | sp, an, trace cpx, gl          |
|                    |      |      | 1240          | 18             | sp, an, cpx, gl                |
|                    |      |      | 1235          | 48             | sp, an, cpx, mel, gl           |
|                    |      |      | 1220          | 72             | fritted cake, sp, an, cpx, mel |
|                    |      |      | 1200          | 72             | loose powder, sp, an, cpx, mel |
| 40                 | 50   | 10   | 1335          | 2              | sp, gl                         |
|                    |      |      | 1330          | 2              | sp, an, gl                     |
|                    |      |      | 1275          | 22             | sp, an, gl                     |
|                    |      |      | 1270          | 18             | sp, an, mel, gl                |
|                    |      |      | 1240          | 18             | sp, an, mel, gl                |
|                    |      |      | 1235          | 48             | sp, an, mel, cpx, gl           |
|                    |      |      | 1220          | 72             | fritted cake, sp, an, mel, cpx |
|                    |      |      | 1200          | 72             | loose powder, sp, an, mel, cpx |
| 70                 | 15   | 15   | 1290          | 2              | cpx, gl                        |
|                    |      |      | 1200          | 336            | barely fritted cake, cpx only  |
| 55                 | 30   | 15   | 1270          | 2              | gl                             |
|                    |      |      | 1265          | 16             | an, gl                         |
|                    |      |      | 1260          | 12             | an, cpx, gl                    |
| 70                 | 10   | 20   | 1305          | 1              | gl                             |
|                    |      |      | 1300          | 2              | cpx, gl                        |
|                    |      |      | 1200          | 72             | lose powder, cpx only          |
| 60                 | 20   | 20   | 1275          | 2              | gl                             |
|                    |      |      | 1270          | 18             | cpx, gl                        |
|                    |      |      | 1240          | 46             | cpx, trace an, trace mel, gl   |
| 50                 | 30   | 20   | 1300          | 15             | gl                             |
|                    |      |      | 1295          | 2              | trace sp, gl                   |
|                    |      |      | 1285          | 2              | sp, gl                         |
|                    |      |      | 1280          | 17             | sp, trace an, gl               |
|                    |      |      | 1270          | 15             | sp, an, gl                     |
|                    |      |      | 1265          | 16             | cpx, an, sp, gl                |
| 40                 | 40   | 20   | 1375          | 16             | gl                             |
|                    |      |      | 1370          | 2              | sp, gl                         |
|                    |      |      | 1335          | 16             | sp, gl                         |
|                    |      |      | 1330          | 2              | sp, an, gl                     |
|                    |      |      | 1260          | 24             | sp, an, gl                     |
|                    |      |      | 1255          | 24             | sp, an, cpx, gl                |
|                    |      |      | 1245          | 48             | sp, an, cpx, gl                |
|                    |      |      | 1240          | 18             | sp, an, cpx, mel, gl           |
| 35                 | 45   | 20   | 1325          | 18             | sp, gl                         |
|                    |      |      | 1320          | 18             | sp, an, gl                     |
|                    |      |      | 1240          | 168            | sp, an, gl                     |
|                    |      |      | 1235          | 168            | sp, an, cpx, mel, gl           |

Table 1. continued

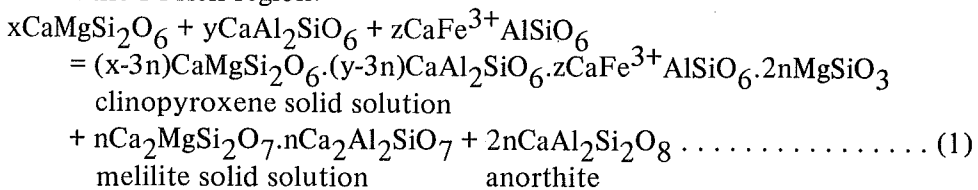
| Di | Composition (wt.%) |      | Temp.<br>(°C) | Time<br>(hrs.) | Results                               |
|----|--------------------|------|---------------|----------------|---------------------------------------|
|    | CaTs               | FATs |               |                |                                       |
| 52 | 25                 | 23   | 1270          | 2              | gl                                    |
|    |                    |      | 1265          | 16             | cpx, gl                               |
|    |                    |      | 1240          | 96             | cpx, trace an, gl                     |
|    |                    |      | 1230          | 96             | cpx, an, mel, gl                      |
| 50 | 25                 | 25   | 1285          | 2              | gl                                    |
|    |                    |      | 1280          | 16             | trace sp, gl                          |
|    |                    |      | 1260          | 18             | sp, gl                                |
|    |                    |      | 1255          | 46             | sp, cpx, gl                           |
|    |                    |      | 1200          | 36             | loose powder, cpx, mel, an            |
| 60 | 10                 | 30   | 1270          | 2              | gl                                    |
|    |                    |      | 1265          | 16             | cpx, gl                               |
|    |                    |      | 1200          | 72             | barely fritted cake, cpx only         |
| 55 | 15                 | 30   | 1265          | 2              | gl                                    |
|    |                    |      | 1260          | 2              | cpx, gl                               |
| 50 | 20                 | 30   | 1270          | 2              | gl                                    |
|    |                    |      | 1265          | 16             | cpx, gl                               |
|    |                    |      | 1200          | 72             | loose powder, cpx only                |
| 48 | 22                 | 30   | 1280          | 6              | gl                                    |
|    |                    |      | 1275          | 5              | sp, gl                                |
|    |                    |      | 1265          | 72             | sp, gl                                |
|    |                    |      | 1260          | 16             | cpx, gl                               |
| 40 | 30                 | 30   | 1375          | 16             | gl                                    |
|    |                    |      | 1370          | 2              | trace sp, gl                          |
|    |                    |      | 1295          | 2              | sp, an, gl                            |
|    |                    |      | 1265          | 18             | sp, an, gl                            |
|    |                    |      | 1260          | 18             | sp, an, cpx, gl                       |
|    |                    |      | 1200          | 336            | barely fritted cake, sp, an, cpx, mel |
| 50 | 10                 | 40   | 1275          | 15             | gl                                    |
|    |                    |      | 1270          | 15             | cpx, gl                               |
|    |                    |      | 1200          | 72             | barely fritted cake, cpx only         |
| 47 | 13                 | 40   | 1280          | 6              | gl                                    |
|    |                    |      | 1275          | 5              | mt, gl                                |
|    |                    |      | 1270          | 16             | mt, gl                                |
|    |                    |      | 1265          | 72             | cpx, gl                               |
| 40 | 20                 | 40   | 1330          | 2              | gl                                    |
|    |                    |      | 1325          | 1              | mt, gl                                |
|    |                    |      | 1285          | 16             | mt, gl                                |
|    |                    |      | 1280          | 44             | mt, cpx, gl                           |
|    |                    |      | 1275          | 15             | mt, cpx, gl                           |
|    |                    |      | 1270          | 15             | px, gl                                |
| 40 | 10                 | 50   | 1345          | 1              | gl                                    |
|    |                    |      | 1340          | 2              | trace mt, gl                          |
|    |                    |      | 1285          | 16             | mt, gl                                |
|    |                    |      | 1280          | 44             | cpx, gl                               |

gl, glass; cpx, clinopyroxene; an, anorthite; mel, melilite; sp, spinel; mt, magnetite.

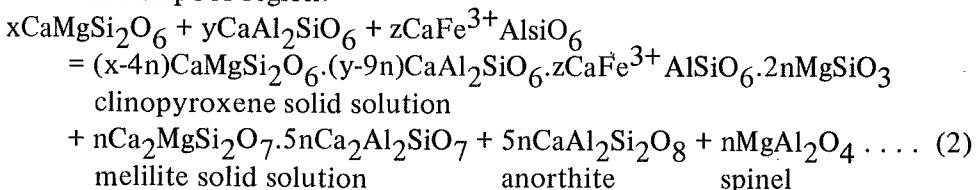
*Phase equilibrium diagrams:* The phase equilibrium diagram at the liquidus temperature is given in Fig. 1. Clinopyroxene<sub>ss</sub> (ss: solid solution), anorthite, spinel<sub>ss</sub>, and magnetite<sub>ss</sub> are encountered as the primary phases. In the liquidus diagram there are two points showing four-phase assemblage. One, at 1250° ± 5°C, shows the liquid coexisting with clinopyroxene<sub>ss</sub>, anorthite, and spinel<sub>ss</sub> and the other, at 1270° ± 5°C, shows the liquid coexisting with clinopyroxene<sub>ss</sub>, magnetite<sub>ss</sub>, and spinel<sub>ss</sub>. These points, however, are neither eutectic nor piercing points because of the nature of the six-component system at the liquidus temperature.

Sections with 10, 20, and 30 wt.% FATs are shown in Figs. 2, 3, and 4. Clinopyroxene<sub>ss</sub>, melilite<sub>ss</sub>, anorthite, and spinel<sub>ss</sub> are encountered as crystalline phases through out the three sections. The maximum phase assemblage is clinopyroxene<sub>ss</sub> + melilite<sub>ss</sub> + anorthite + spinel<sub>ss</sub> + liquid at the solidus temperatures showing univariant phase assemblage in the five-component system. Since at higher temperature the reaction Fe<sub>2</sub>O<sub>3</sub> = 2FeO + 1/2O<sub>2</sub> takes place in air, the join is a part of the six-component system Fe-O-CaO-MgO-Al<sub>2</sub>O<sub>3</sub>-SiO<sub>2</sub>. At lower temperature, however, this reaction does not occur and the join can be treated as a five-component system MgO-CaO-Fe<sub>2</sub>O<sub>3</sub>-Al<sub>2</sub>O<sub>3</sub>-SiO<sub>2</sub>. In these sections, the phase assemblages clinopyroxene<sub>ss</sub> + anorthite + melilite<sub>ss</sub> in the Di-rich region and clinopyroxene<sub>ss</sub> + anorthite + melilite<sub>ss</sub> + spinel<sub>ss</sub> in the Di-poor region are found as the final phase assemblages at the subsolidus temperatures. These assemblages are expected from the following reactions with the formation of the complicate solid solutions of clinopyroxene and melilite.

In the Di-rich region:



In the Di-poor region:



This fact and the equations indicate that the crystallization ceases on the divariant surface or the univariant line before invariant point is reached, because clinopyroxene and melilite form complicate solid solutions.

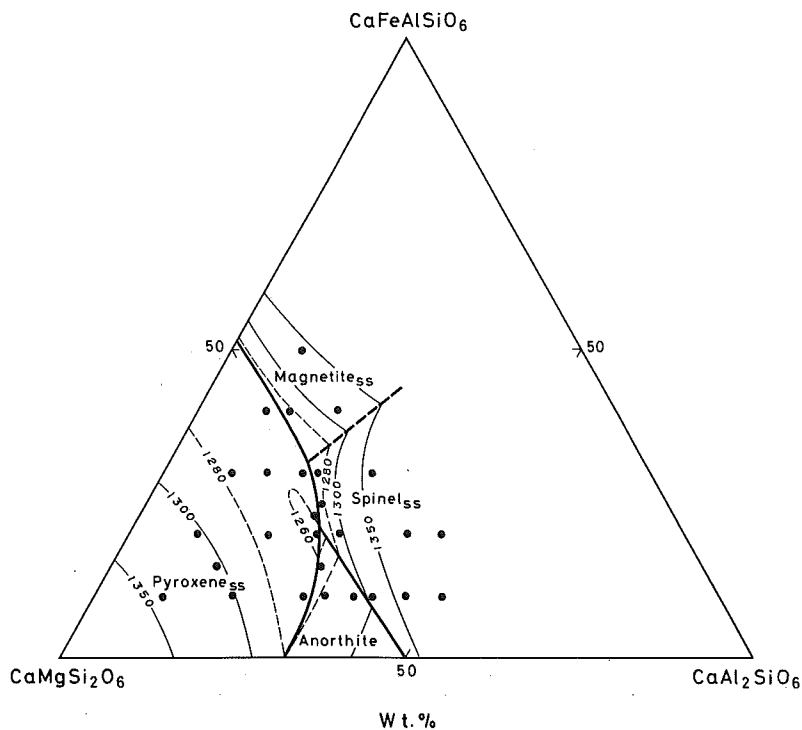


Fig. 1 Liquidus diagram of the join  $\text{CaMgSi}_2\text{O}_6$ - $\text{CaAl}_2\text{SiO}_6$ - $\text{CaFe}^{3+}\text{AlSiO}_6$ .

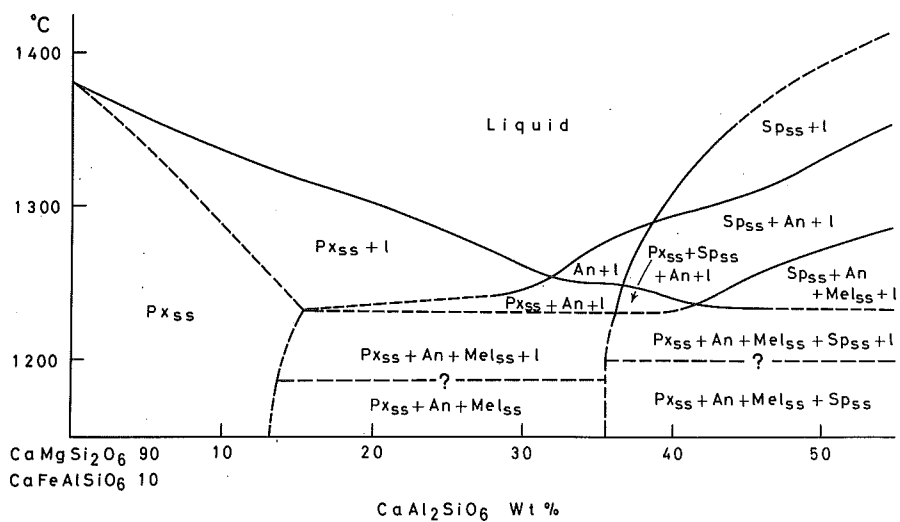


Fig. 2 Phase equilibrium diagram of 10%  $\text{CaFe}^{3+}\text{AlSiO}_6$  section.

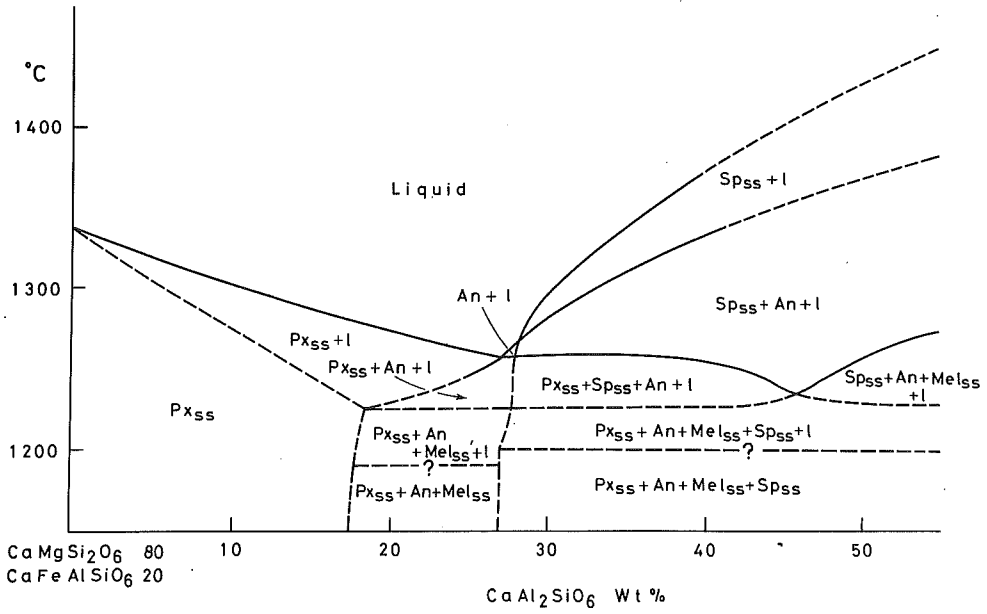


Fig. 3 Phase equilibrium diagram of 20%  $\text{CaFe}^{3+}\text{AlSiO}_6$  section.

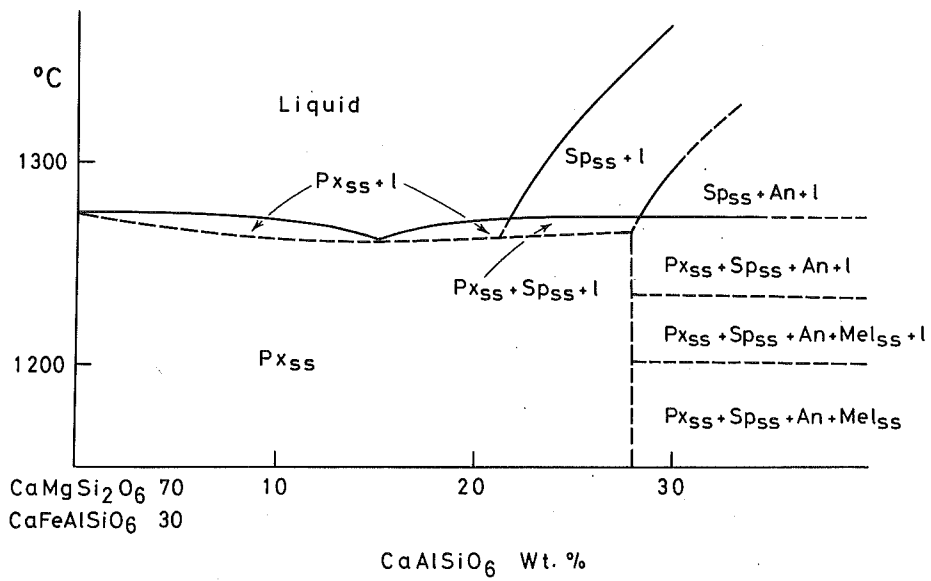


Fig. 4 Phase equilibrium diagram of 30%  $\text{CaFe}^{3+}\text{AlSiO}_6$  section.



10 and 20 wt.% FATs sections are similar to each other. In the both sections five-phase assemblage clinopyroxene<sub>SS</sub> + anorthite + melilite<sub>SS</sub> + spinel<sub>SS</sub> + liquid is surrounded by three four-phase assemblages, clinopyroxene<sub>SS</sub> + melilite<sub>SS</sub> + anorthite + liquid, clinopyroxene<sub>SS</sub> + anorthite + spinel<sub>SS</sub> + liquid, and anorthite + melilite<sub>SS</sub> + spinel + liquid, which are divariant in five-component system. The relationship between the five-phase assemblage and the four-phase assemblages is shown in Fig. 5. Of the four four-phase assemblages, the assemblage clinopyroxene + melilite + spinel + liquid, which is confirmed in the system CaO-MgO-Al<sub>2</sub>O<sub>3</sub>-SiO<sub>2</sub> as a univariant line (O'Hara and Biggar, 1969), was not found in the present investigation.

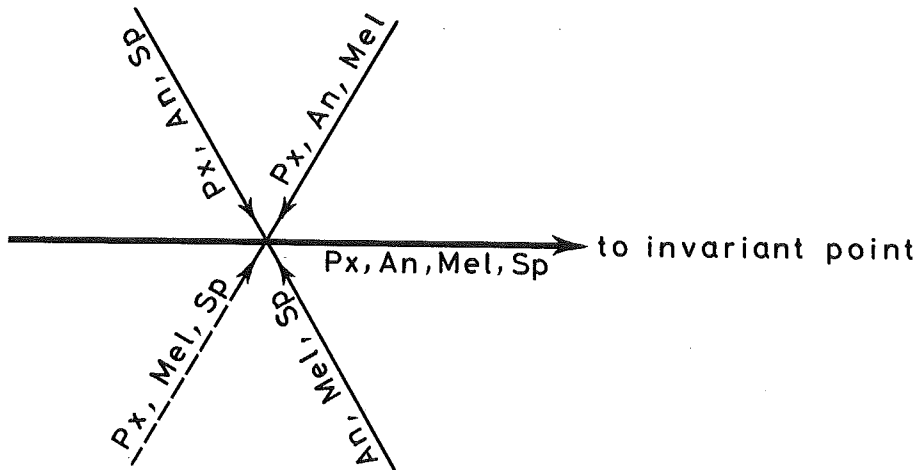


Fig. 5 Relationship between four four-phase assemblages and a five-phase assemblage. Liquid phase is eliminated.

The four-phase assemblage clinopyroxene<sub>SS</sub> + anorthite + melilite<sub>SS</sub> + liquid is no longer stable in 30% FATs section. Three three-phase assemblages clinopyroxene<sub>SS</sub> + anorthite + liquid, anorthite + spinel<sub>SS</sub> + liquid, and clinopyroxene<sub>SS</sub> + spinel<sub>SS</sub> + liquid were confirmed in the present system. The assemblage clinopyroxene<sub>SS</sub> + anorthite + liquid is not stable and the assemblage clinopyroxene<sub>SS</sub> + spinel<sub>SS</sub> + liquid is present in 30% FATs section.

*Limit of clinopyroxene solid solution at subsolidus temperature:* Hijikata and Onuma (1969) found that diopside and FATs forms complete solid solution below 1265°C. Schairer and Yoder (1970) showed that the maximum solubility of CaTs in diopside is about 12 wt.% at 1250°C. Through the

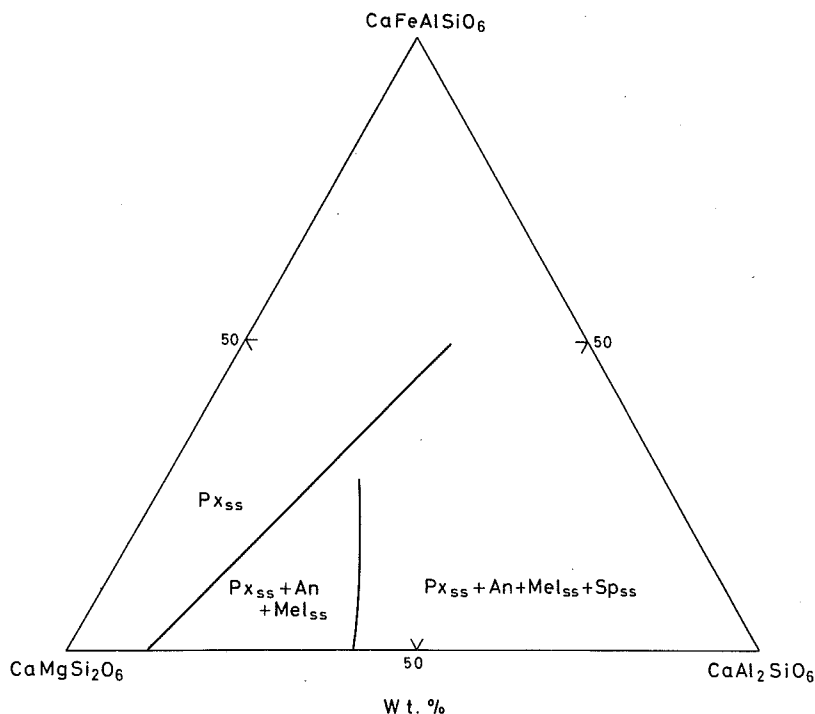


Fig. 6 Phase assemblages at subsolidus region.

sections 10, 20, and 30% FATs, the clinopyroxene solid solution area increases with the increase of FATs contents, that is, maximum solubility of CaTs in diopside is 15 wt.% at about 1230°C in 10% section, 18 wt.% at about 1225°C in 20% section, and 28 wt.% at 1270°C in 30% section with solid solution minimum at 1265°C and at  $\text{Di}_{48}\text{CaTs}_{22}$  FATs<sub>30</sub>. It is noticed in Fig. 6 that the limit of the clinopyroxene solid solution at 1250°C increases with increasing FATs.

*Crystalline phases:* Clinopyroxene<sub>ss</sub>, anorthite, melilite<sub>ss</sub>, spinel<sub>ss</sub>, and magnetite<sub>ss</sub> are crystalline phases encountered in the present system. Clinopyroxene<sub>ss</sub> forms prismatic crystals near liquidus but forms rounded grains in subsolidus region. They are always bright yellow in color. X-ray diffraction patterns of the clinopyroxene<sub>ss</sub> crystallized at 1200°C for 72 hours in 10% FATs section are shown in Fig. 7. It is evident that the 002 peak shifts to lower angles and  $\Delta 2\theta_{221-002}$  becomes larger with increasing CaTs, indicating that the clinopyroxene is not pure diopside but solid solution as shown in equations (1) and (2). The relationship between  $\Delta 2\theta_{221-002}$  and phase assemblage is shown

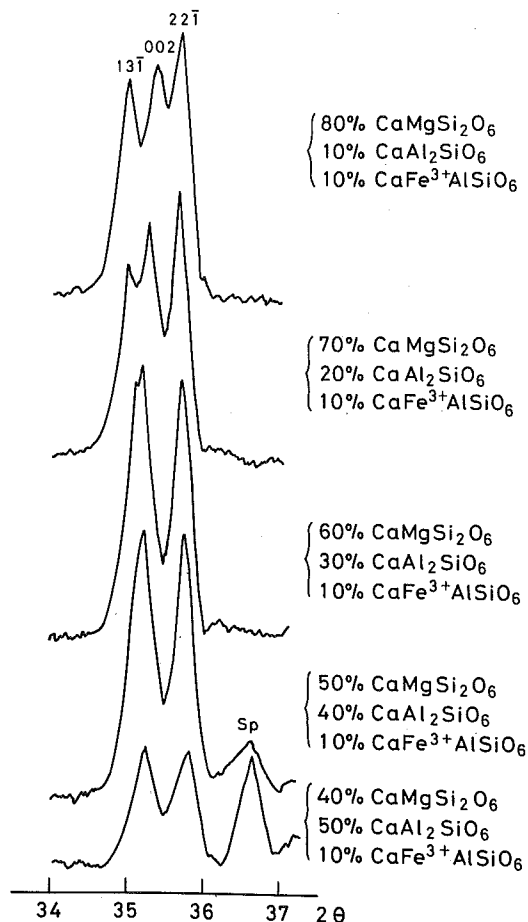


Fig. 7 X-ray diffraction patterns of the clinopyroxene solid solutions crystallized at 1200°C for 72 hours in 10%  $\text{CaFe}^{3+}\text{AlSiO}_6$  section, showing the shift of the 002.

in Fig. 8.  $\Delta 2\theta_{221-002}$  increases with increasing CaTs in the phase assemblage clinopyroxene<sub>ss</sub> + melilite<sub>ss</sub> + anorthite and remains at constant value in the assemblage clinopyroxene<sub>ss</sub> + melilite<sub>ss</sub> + anorthite + spinel<sub>ss</sub>. Since four-phase assemblage is divariant in five-component system, the composition of one of four crystalline phases is variable at constant temperature. Therefore, melilite<sub>ss</sub> or spinel<sub>ss</sub> has variable composition. Since melilite<sub>ss</sub> occurs at lower temperature region together with other minute crystals, sometimes it was difficult to identify this mineral under the microscope. The strongest peak of melilite obtained in the present study in X-ray diffraction has

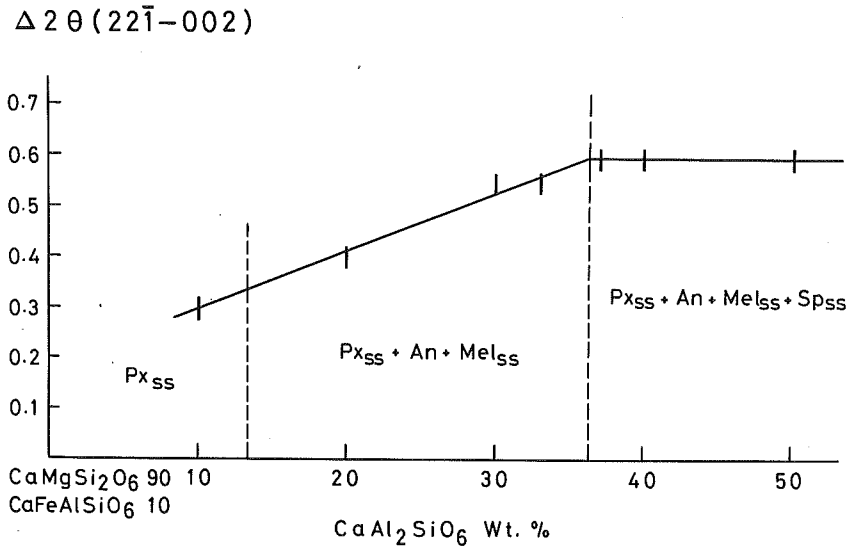


Fig. 8 Change of  $\Delta 2\theta_{221-002}$  of the clinopyroxene solid solutions crystallized at  $1200^\circ\text{C}$  for 72 hours in 10%  $\text{CaFe}^{3+}\text{AlSiO}_6$  section.

value between  $31.1^\circ$  and  $31.3^\circ$  in  $2\theta$ , suggesting that melilite<sub>ss</sub> consists of akermanite and gehlenite as indicated in the equations (1) and (2). Anorthite occurs as needles or platy crystals having low birefringence and 204 reflection is  $27.92^\circ$  in  $2\theta$ , indicating that anorthite is pure compound but not solid solution. Spinel<sub>ss</sub> forming small octahedral crystals is almost colorless in the FATs-poor region but is pale brown in color in the FATs-rich region. This color may be ascribed to substitution of  $\text{Fe}^{3+}$  in spinel<sub>ss</sub> and becomes deeper with increasing FATs. Magnetite<sub>ss</sub> was found only at the liquidus temperatures and subliquidus temperatures in the FATs-rich region as octahedral form with distinct crystal faces and probably is solid solution with spinel molecule. Huchenholz *et al.* (1968) analysed the magnetite<sub>ss</sub> which appears at the liquidus temperatures in the analogous system diopside-FTs and found that this magnetite<sub>ss</sub> contains considerable amount of Mg. This may be also the case in the magnetite<sub>ss</sub> in the present investigation. It is estimated that Al is also incorporated in magnetite<sub>ss</sub>.

### The Join Bearing on Fassaitic Pyroxene

It is known that clinopyroxenes from alkalic rock are higher in Al and Ti contents than those from tholeiite basalt, and these ions are incorporated in diopside as CaTs and Tp (Kushiro, 1960 and Yagi and Onuma, 1967). The substitution of CaTs in diopside, according to Clark *et al.* (1962), is favored by high pressure, while Yagi and Onuma (1967) have shown that Ti-rich diopside decomposes into Ti-poor diopside and perovskite ( $\text{CaTiO}_3$ ) at 10 kbar.

The clinopyroxene from understaturated alkalic rocks, such as nephelinite and melilitite, is rich not only in CaTs but also in Tp, FTs, and FATs, and includes small amount of acmite molecule, usually less than 5%. The clinopyroxene in a kalsilite-bearing olivine melilitite of Nyragongo, East Africa (Sahama and Meyer, 1958) includes 21.4% total Tschermak's molecule ( $\text{Ts} = \text{CaTs} + \text{FTs} + \text{FATs} + \text{Tp}$ ) and that in a melilitite nepheline dolerite of Scawt Hill, Antrin (Tilley and Harwood, 1931) 30.7%, respectively. Therefore, these clinopyroxenes are fassaitic pyroxenes with the substitution of Al for Si. Huchenholtz (1974), in a review on the chemical composition of the pyroxenes in alkalic basalts from various localities, pointed out that when  $\text{Na} < \text{Fe}^{3+} + \text{Al}$  the pyroxenes are rich in total Ts and fassaitic rather than acmitic and quoted Hibsh's report (1943) showing that the fassaitic augite from a leucite tephrite of the Central Mountain of Bohemia contains 30% total Ts, of which FTs content is 58%.

The present investigation seems to agree with these facts. The mixture  $\text{Di}_{70}\text{CaTs}_{15}\text{FATs}_{15}$  crystallizes as single phase of clinopyroxene, indicating that this clinopyroxene contains 30% total Ts. The experimental results show that the solubility of total Ts in diopside considerably increases even at lower pressure, when oxygen partial pressure is high enough to form FATs. Diopside and FATs form a complete solid solution series in air at 1 atm. (Hijikata and Onuma, 1969), but all of these solid solutions richer in FATs than  $\text{Di}_{90}\text{FATs}_{10}$  decompose into hedenbergitic pyroxene, melilitite and hercynite above  $1000^\circ\text{C}$  at lower oxygen fugacity, say  $10^{-11}$  (Onuma and Oba, unpublished data). Onuma and Hariya (unpublished data) showed that the clinopyroxene crystallized from the mixture  $\text{Di}_{70}\text{CaTs}_{15}\text{FATs}_{15}$  decomposes into diopsidic pyroxene, garnet, and oxide at 10 kbar. These experimental results and chemical composition of natural fassaitic pyroxene suggest that the volcanic rocks including fassaitic pyroxene, such as melilitite, nephelinite, basanite, tephrite, and other alkalic rocks, were formed at rather low pressure, less than 10 kbar and at higher oxygen pressure.

Yagi (1966) suggested that when oxygen partial pressure in the magma is higher pyroxene becomes acmitic, while lower pyroxene includes more

hedenbergite molecule. However, if a magma is poor in Na and rich in Ca such as melilitite, pyroxene crystallizing from it incorporates Ts which is rich in Ca, and when nepheline and melilite crystallize together with pyroxene Na is incorporated in these minerals and pyroxene contains only small amount of Na.

Taking these discussions into account, pyroxenes from alkalic rocks rather low in Na and high in Ca can be described in terms of the four molecules Di, CaTs, FATs, and Tp, and the system Di-CaTs-FATs-Tp is relevant for understanding the crystallization of pyroxene in such alkalic rocks. It is noted in Fig. 9 that the estimated pyroxene solid solution volume at subsolidus in the system Di-CaTs-FATs-Tp expands towards the FATs corner and that the content of total Ts in diopside may exceed 30%, which is a maximum value in the natural fassaitic pyroxene in alkalic volcanic rocks.

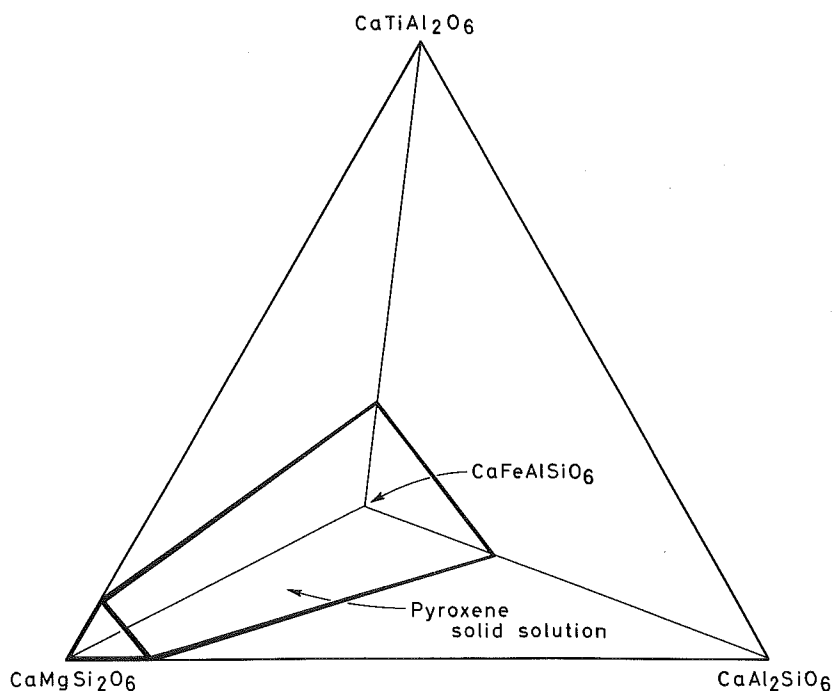


Fig. 9 Estimated clinopyroxene solid solution volume in the system  $\text{CaMgSi}_2\text{O}_6$ - $\text{CaAl}_2\text{SiO}_6$ - $\text{CaFe}^{3+}\text{AlSiO}_6$ - $\text{CaTiAl}_2\text{O}_6$  at atmospheric pressure.

### Acknowledgement

Mr. S. Terada of Hokkaido University helped the authors in the laboratory and in preparation of figures. Part of the cost for the present study was defrayed by a Grant for Scientific Research from the Ministry of Education of Japan, and by a fund from the Mitsubishi Foundation.

*References*

- Clark, S. P., J. F. Schairer, and J. Neufville (1962): Phase relations in the system  $\text{CaMgSi}_2\text{O}_6\text{-CaAl}_2\text{SiO}_6$  at low and high pressure. *Carnegie Inst. Wash. Year Book*, 61, 59-68.
- Hijikata, K. and K. Onuma (1969): Phase equilibria of the system  $\text{CaMgSi}_2\text{O}_6\text{-CaFe}^{3+}\text{AlSiO}_6$  in air. *Japan. Assoc. Mineral. Petrol. Econ. Geol.*, 62, 209-217.
- Huckenholz, H. G. (1973): The origin of fassaitic augite in the alkali basalt in suite of the Hocheifel area, Western Germany. *Contr. Mineral. Petrol.*, 40, 315-326.
- Huckenholz, H. G., J. F. Schairer, and H. S. Yoder, Jr. (1968): Synthesis and stability of ferri-diopside. *Carnegie Inst. Wash. Year Book*, 66, 335-347.
- Kushiro, I. (1960): Si-Al relations in clinopyroxenes from igneous rocks. *Am. Jour. Sci.*, 258, 548-554.
- O'Hara, M. J. and G. M. Biggar (1969): Diopside + spinel equilibria, anorthite and forsterite reaction relationship in silica-poor liquids in the system  $\text{CaO-MgO-Al}_2\text{O}_3\text{-SiO}_2$  at atmospheric pressure and their bearing on the genesis of melilitites and nephelinites. *Am. Jour. Sci.*, Schairer vol. 267-A, 364-390.
- Onuma, K. and K. Yagi (1971): The join  $\text{CaMgSi}_2\text{O}_6\text{-Ca}_2\text{MgSi}_2\text{O}_7\text{-CaTiAl}_2\text{O}_6$  in the system  $\text{CaO-MgO-Al}_2\text{O}_3\text{-TiO}_2\text{-SiO}_2$  and its bearing on the titanpyroxene. *Mineral. Mag.*, 38, 471-480.
- Sahama, Th. G. and A. Meyer (1958): Exploration du Parc National Albert, 2, *Inst. Parcs Nat. Congo Belge*, pp. 58.
- Schairer, J. F. and H. S. Yoder, Jr. (1970): Critical planes and flow sheet for a portion of the system  $\text{CaO-MgO-Al}_2\text{O}_3\text{-SiO}_2$  having petrological application. *Carnegie Inst. Wash. Year. Book*, 68, 202-214.
- Tilley, C. E. and H. F. Harwood (1931): The dolerite-chalk contact of Scawt Hill, Co. Antrim. The production of basic alkalic rocks by assimilation of limestone by basaltic magma. *Mineral. Mag.*, 22, 439-468.
- Yagi, K. and K. Onuma (1967): The join  $\text{CaMgSi}_2\text{O}_6\text{-CaTiAl}_2\text{O}_6$  and its bearing on the titanaugites. *Jour. Fac. Sci. Hokkaido Univ.*, ser. IV, 13, 463-483.

(Received on Sept. 1, 1974)